CORRELATIONS OF MAGNETIC MICROSTRUCTURE AND ANISOTROPY WITH NOISE SPECTRA FOR CoNi and CoCrTa THIN FILM MEDIA

Mahbub R. Khan, S.Y. Lee, J.L.Pressesky, D.Williams, S.L.Duan, R.D. Fisher and Neil Heiman
Seagate Magnetics, 47001 Benicia Street, Fremont, California 94538, U.S.A.
M.R. Scheinfein, J. Unguris, D.T. Pierce and R.J. Celotta
National Institute of Standards and Technology, Gaithersburg, MD 20899, U.S.A.
Dennis E. Speliotis
Advanced Development Corporation, 8 Ray Avenue, Burlington, MA 01803, U.S.A.

Abstract: This paper reports on two thin film media alloys $Co_{86}Cr_{12}Ta_2$ and $Co_{75}Ni_{25}$ which have very different noise characteristics. The magnetic microstructure of these films was observed with SEMPA. The anisotropy and the rotational hysteresis loss measurements have been made using a torque magnetometer. The distribution of anisotropy field Hk and its width dHk have also been measured, along with its different normalized values. We suggest that the observed magnetic microstructure can be directly correlated with measured readback noise and anisotropy differences.

Introduction

There has recently been much interest in the noise characteristics of recording media [1,2] which has not been completely explained by current theoretical models [1,3-8]. There are reports of noise correlations with anisotropy constant K [4,5], grain boundary segregation and magnetostatic or exchange interactions [6,7], coercive squareness S* [8], rotational hysteresis integral Rh [4], etc. In the previous works [5,8,10], the samples studied had very different bulk magnetic properties. In the present study, CoCrTa and CoNi samples were carefully prepared so that they had very similar parametrics but very different noise characteristics [9]. The magnetic microstructure of these two alloys was observed with Scanning Electron Microscopy with Polarization Analysis (SEMPA) [11,12]. Measurements of the anisotropy and rotational hysteresis loss were made using a torque magnetometer. The observed magnetic microstructure and the measured anisotropy and rotational hysteresis losses for these two alloys can be directly correlated with the measured noise spectra.

Experimental

The $Co_{75}Ni_{25}$ and $Co_{86}Cr_{12}Ta_2$ samples were prepared by DC magnetron sputtering on circumferencially textured 95 mm Al based NiP substrates with a 400 A thick Cr underlayer.

The readback noise measurements were made with a mini-monolithic 3370 slider type Winchester recording head with a gap width of 40 μin and a flying height of 16 μin [9]. The integrated noise voltage was determined by sampling the noise spectrum at 0.25 MHz intervals over a bandwidth of 10 MHz. The write currents and the writing frequency ranged from 2.5 to 100 ma and 2.5 to 12.5 MHz respectively.

The magnetic properties of the alloys were measured using a vibrating sample magnetometer (VSM). The grain structure was obtained using a high resolution SEM. The anisotropy and the rotational hysteresis loss measurements have been made using a Torque magnetometer at a peak field of 14 kOe. In this particular torque magnetometer, the sample remains stationary, and the applied field rotates in the horizontal plane. The torque measurements were performed in the following three directions:

HL: Sample plane horizontal, field parallel to the texture lines at the start, field rotating in the sample plane.
VL: Sample plane vertical, field parallel to the texture lines at the start, field rotating out of sample plane.
VT: Same as VL, but field perpendicular to the texture lines at the start.

The magnetic microstructure of these films was observed using Scanning Electron Microscopy with Polarization Analysis, SEMPA [11,12]. In SEMPA, a focused beam of high energy electrons is scanned across the surface of a sample. The secondary electrons which are excited at the surface by the incident electron beam leave the sample without losing their electron-spin orientation. By spin-analyzing the emitted polarized secondary electrons as the electron beam rasters the sample surface, a map of the net electron spin density results. For most transition metal ferromagnets, this spin density can be directly related to the specimen surface magnetization. With two orthogonal detectors, all three components of the magnetization vector can be measured. The SEMPA samples were prepared by writing with 20 mAop (zero to peak) write current on a DC erased surface with bit densities of 58.8 fcmm (flux changes per millimeter) and 588 fcmm. Prior to observation, the samples were sputter cleaned with 2 keV Ar ions to remove the native oxide.

Results and Discussion

As pointed out in ref [9], much reported work on noise comparisons yields confusing results, because the bulk magnetic properties of the samples are so different. Therefore to eliminate that problem in this paper, we selected two alloys which display very different noise power, but have very similar parametrics. The sputtering process was adjusted such that the magnetic and recording properties are nearly the same for the two alloys (Table 1).

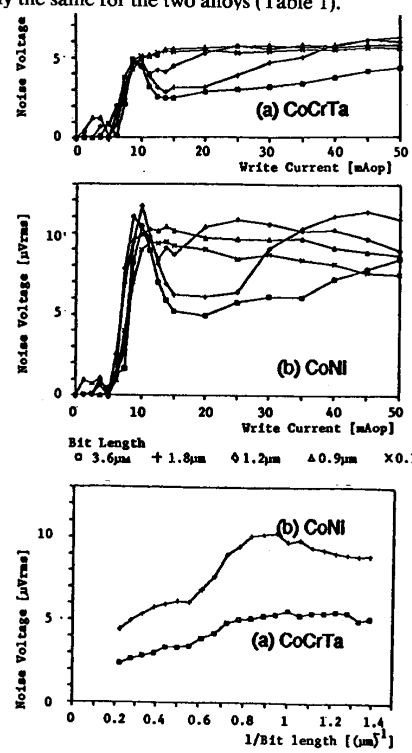

Fig. 1: (a) Noise spectra from $Co_{86}Cr_{12}Ta_2$ and (b) $Co_{75}Ni_{25}$ films. (c) Noise voltage as a function of frequency. SEMPA samples were written at 20 mAop (fig 1a,b) and 0.588 $(\mu m)^{-1}$ (fig.1c)

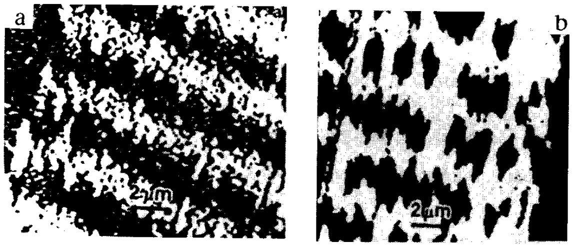

Fig. 2: (a) SEMPA image of $Co_{86}Cr_{12}Ta_2$ and (b) $Co_{75}Ni_{25}$ films. The images are of the magnetization component along the track.

The integrated noise voltage as a function of the write current (at different frequencies or bit lengths) is shown in Fig. 1a and 1b for CoCrTa and CoNi respectively. Fig. 1c shows the noise as a function of frequency or inverse bit length for the optimum write current of 20 mA o-p. It is obvious that of the two alloys the CoNi has significantly higher noise. It also shows the onset of superlinear increase in noise [1] for CoNi at about the density where SEMPA samples were written. CoCrTa samples do not show this superlinear noise behavior.

The SEMPA images of the written bits in the CoCrTa and CoNi films are shown in Fig 2a 2b respectively. The average track width for both samples are about 17 μm and the average bit spacing is about 1.7 μm . The ratio of magnetization Ms for the two samples as obtained from SEMPA is 1.65 and compares very well with 1.62 obtained from VSM measurements. In these SEMPA images, the component of magnetization along the tracks is imaged. White (black) represents magnetization pointing forward (back) along the track in the plane of the figure. Here the CoCrTa domains or bits are well separated by jagged boundaries. The domains are oriented primarily in the direction along the track, with a minimum amount of edge curling at the domain boundaries. For CoNi specimen, the bits are cross linked, and the neighboring domains are bridged together. Also, the track edges are poorly defined.Although the T50 for isolated pulses are a little narrower for CoNi (Table 1), the cross-bit linkages correlate well with the superlinear noise behaviour at higher density.

The torque results are summarized in Table 2. The highest torque is obviously VL because it incorporates both the sample shape and the in-plane orientation effects. The total net anisotropy (K) can be obtained from:

$$K = 2\pi Ms^2 + Ku = Lpp / 2V \qquad \text{(Eq. 1)}$$

where Ku is the film uniaxial anisotropy (in the plane if Ku > 0 and out of the plane if Ku < 0), V is the sample volume and Lpp is the peak to peak torque. The VL torques (Fig. 3) indicates the presence of other harmonics, even at the 14 kOe field. To obtain the correct values of the anisotropy constants, we must extrapolate to infinite field

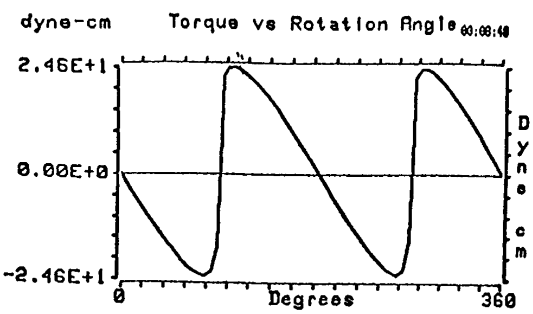

Fig. 3: Torque vs Rotation Angle for CoNi sample.

Table 1: Magnetic and recording properties of $Co_{86}Cr_{12}Ta_2$ and $Co_{75}Ni_{25}$ films.

	CoCrTa	CoNi
Thickness (μm)	0.07	0.043
M_s (emu/cm^3)	660	1070
H_c (Oe)	693	730
M_r*t (memu/cm^2)	3.80	4.02
S	0.820	0.874
S*	0.893	0.903
Eo o-p(μV)	342	365
T50 (nsec)	206	204

[13]. This is shown in Fig 4. The x-intercept gives the extrapolated value of L and we get K by using Eq. 1. Lop is the zero to peak of the fundamental of the torque curve and Is is the total magnetic moment of the sample (Table 2).

Several models [4,8] for noise suggest that if K is low, the magnetization reversal in the transition regions can in part take place out of the film plane. If, however, K is high, magnetization reversal must stay more in plane, resulting in a wide transition with zigzags and higher modulation noise. Therefore, this model leads to the conclusion that the modulation (zigzag-type transition noise) is lower if K is lower. This prediction is consistent with the measured K values (Table 2) as well as the SEMPA images (Fig. 2). The wall width is a factor of 2 smaller than the resolution of the present SEMPA apparatus and therefore the z-component of magnetization within the wall of the transition region, which would provide direct confirmation of this model, could not be measured.

The rotational hysteresis loss (Wr) and the rotational hysteresis integral (Rh) are obtained from:

$$W_r\,(H) = \int_0^{2\pi} L\, d\Theta \qquad R_h = \int_0^{\infty} [W_r(H)/M_s]\, d(1/H) \qquad \text{---(Eq. 2)}$$

The distribution of rotational hysteresis losses are quite different for the two samples [Fig. 5]. The Rh values are obtained by integrating the areas under the curves in Fig. 5. By extrapolating Fig. 5 at higher fields we get the anisotropy field Hk directly from the x-intercept. This Hk is actually $(Hk)_{max}$ for which Wr(H) is zero. The high field points in Fig. 5 have low Wr(H) values which approaches the noise level and therefore were omitted during extrapolation. The Rh and Hk values are shown in Table 2. The distribution of Hk for both samples have also been measured by a technique described in ref [14]. The width of this distribution, dHk, and its normalized values w.r.t. Hc and Hr etc. are shown in Table 3. The Hc and Hr are the intrinsic and remanent coercivities respectively. The differences in these parameters (viz., Wr(H), Rh, Hk, dHk and its various normalized values) and their correlations with noise are still under investigation.

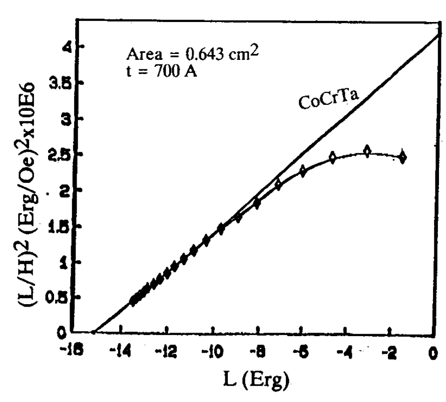

Fig. 4: Torque (L) vs. (L/H)2. The extrapolated X-intercept gives the anisotropy constant K.

Table 2: Torque and Anisotropy Characteristics of CoCrTa and CoNi Films

Sample	Dir. of measure.	Rh	Hk (kOe)	K erg/cc	Ku erg/cc	Q = $Ku/2\pi Ms^2$	Lpp dyne-cm	Lop dyne-cm	Lpp/Is (Oe)
CoCrTa	HL	1.57	3.75				2.86	1.41	953
	VL			3.37E6	5.95E5	0.213	31.9	14.7	10633
	VT						29.3	13.6	9767
CoNi	HL	1.63	2.42				5.11	2.55	1721
	VL			9.16E6	1.61E6	1.340	48.3	20.7	16263
	VT						42.8	19.1	14276

Table 3: Distribution of Hk for CoCrTa and CoNi films

Sample	Hk	dHk	dHk/dHc	dHk/dHr	$dHk/Hr_{\parallel}$	$dHk/Hr_{\perp}$	$dHk/Hc_{\parallel}$	$dHk/Hc_{\perp}$
CoCrTa	3750	1180	24.8	31.9	1.44		1.65	2.07
CoNi	2420	1128	23.0	23.1	1.64		1.45	2.45

Conclusion

Samples of CoCrTa and CoNi films, specially prepared to have very similar magnetic and recording properties, show much higher modulation noise for the CoNi sample.

The SEMPA images of the recording transitions provide the first and direct demonstration that the differences in modulation noise correlate to differences in the nature of the zig-zag transitions.

These SEMPA images of highest spatial resolution ever for recording transitions show that CoCrTa domains or bits are well separated by jagged boundaries , whereas, CoNi bits are cross-linked and neighboring bits are bridged together. The images also show that the track edges of the noisier CoNi film are less well defined.

CoNi sample shows superlinear noise behavior as opposed to CoCrTa and correlates well with cross-bit linkages observed in SEMPA image [1,16].

Torque measurements on these samples show that the net anisotropy constant K is larger for CoNi than for CoCrTa. This result supports the anisotropy model which predicts that higher K requires the magnetization to remain more in plane during reversal resulting in a wider transition with zig-zags and higher noise, whereas for lower K, magnetization reversal can in part take place out of the film plane, resulting in narrower transition and lower noise.

Rotational hysteresis measurements show that Rh is similar, but Hk_{max} and the distribution of Wr(H) are different for the two samples. The distribution of Hk, its width dHk, and various normalized values of dHk are different as well. The differences in these parameters may also contribute for the noise difference but are the subjects of further studies at this time.

Other interpretations of these results are also possible. For example, the differences in the noise characteristics of the two alloys could be related as well to the structure of the grain boundaries within the films. The SEM micrographs in Fig. 6 shows that the grains of CoCrTa film are isolated with clear grain boundaries, whereas, the CoNi film shows closely packed grains with less well defined grain boundaries, though the differences are not dramatic. In CoNi, the Ni forms solid solutions with Co [15], but in CoCrTa, the Cr has been shown to segregate towards grain boundaries [6]. Exchange interactions could therefore be somewhat weaker between grains in CoCrTa, resulting in lesser cross-bit linkages and lower noise than CoNi, although S* is clearly similar in both films.

Acknowledgements: The SEMPA effort is supported in part by the Office of Naval Research.

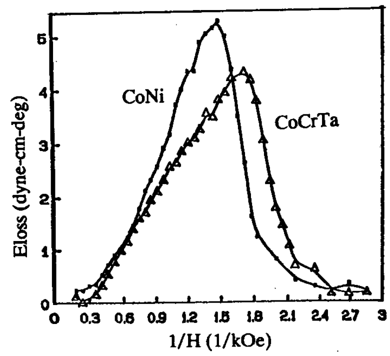

Fig. 5: Rotational hysteresis loss (Wr) vs. 1/H for CoCrTa and CoNi samples.

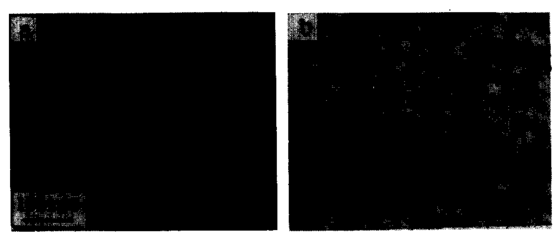

Fig. 6: SEM micrographs for (a) CoCrTa and (b) CoNi films.

References

[1] N. Belk et.al., IEEE Trans. Magn., 21, 1350 (1985).
[2] R.A. Baugh et. al., IEEE Trans. Magn.,19, 1722 (1983).
[3] A. M. Barany et.al., IEEE Trans. Magn., 23, 1776 (1987).
[4] D.E.Speliotis, IEEE Trans. Magn., 24, 2979 (1988).
[5] Y. Shiroishi et. al., IEEE Trans. Magn.,24,2730 (1988).
[6] D.J.Rogers et. al., IEEE Trans. Magn., 25, 4180 (1989).
[7] T. Chen et. al., IEEE Trans. Magn.,24, 2700 (1988).
[8] I. L. Sanders et. al., J. Appl. Phys., 65, 1234 (1989).
[9] S.Y. Lee et.al.,IEEE Trans. Magn., 26, 121 (1990)
[10] T. Kawanabe et. al., IEEE Trans. Magn., 24, 2721 (1988).
[11] G.G. Hembree et.al., Scanning Microscopy Supplement 1, 229 (1987), Scanning Microscopy International.
[12] M.R. Scheinfein et.al., Rev. Sci. Instrum. (in press).
[13] H. Miyajima, et. al., J. Appl. Phys., 47, 4669 (1976).
[14] D.E.Speliotis, Paper HB-11, This conference.
[15] P. M. Hansen, Constitution of Binary Alloys, Mc Graw Hill, p.466 (1958).
[16] T.C.Arnoldussen et.al., IEEE Trans. Magn., 22,889 (1986)